



Zhang, S. Y., Li, Y. Y., Jiang, J. Z., Neild, S. A., & Macdonald, J. H. G. (2019). A methodology for identifying optimum vibration absorbers with a reaction mass. *Proceedings of the Royal Society A: Mathematical, Physical and Engineering Sciences*, 475(2228), [20190232].
<https://doi.org/10.1098/rspa.2019.0232>

Peer reviewed version

Link to published version (if available):
[10.1098/rspa.2019.0232](https://doi.org/10.1098/rspa.2019.0232)

[Link to publication record in Explore Bristol Research](#)
PDF-document

This is the author accepted manuscript (AAM). The final published version (version of record) is available online via The Royal Society at <https://royalsocietypublishing.org/doi/10.1098/rspa.2019.0232> . Please refer to any applicable terms of use of the publisher.

University of Bristol - Explore Bristol Research

General rights

This document is made available in accordance with publisher policies. Please cite only the published version using the reference above. Full terms of use are available:
<http://www.bristol.ac.uk/pure/about/ebr-terms>



Article submitted to journal

Subject Areas:

passive vibration control, network synthesis

Keywords:

reaction mass, inerter, passive vibration absorber, restricted complexity realisation

Author for correspondence:

Jason Zheng Jiang
e-mail: z.jiang@bristol.ac.uk

A methodology for identifying optimum vibration absorbers with a reaction mass

Sara Ying Zhang^{1,2}, Yi-Yuan Li², Jason Zheng Jiang², Simon A. Neild^{2,3} and John H.G. Macdonald³

¹ Institute of Urban Smart Transportation & Safety Maintenance, Shenzhen University, Shenzhen 518060, China

² Department of Mechanical Engineering, University of Bristol, Queen's Building, University Walk, Bristol, UK

³ Department of Civil Engineering, University of Bristol, Queen's Building, University Walk, Bristol, UK

Tuned mass dampers (TMDs), in which a reaction mass is attached to a structural system via a spring-parallel-damper connection, are commonly used in a wide range of applications to suppress deleterious vibrations. Recently, a mass-included absorber layout with an inerter element, termed the tuned mass damper inerter (TMDI), was introduced, showing significant performance benefits on vibration suppression. However, there are countless mass-included absorber layouts with springs, dampers and inerters, which could potentially provide more preferred dynamic properties. Currently, because there is no systematic methodology for accessing them, only an extremely limited number of mass-included absorber layouts have been investigated. This paper proposes an approach to identify optimum vibration absorbers with a reaction mass. Using this approach, a full class of absorber layouts with a reaction mass and a pre-determined number of inerters, dampers and springs connected in series and parallel, can be systematically investigated using generic Immittance-Function-Networks. The advantages of the proposed approach are demonstrated via a three degree-of-freedom structure example.

1. Introduction

The concept of attaching an additional reaction mass to

© The Authors. Published by the Royal Society under the terms of the Creative Commons Attribution License <http://creativecommons.org/licenses/by/4.0/>, which permits unrestricted use, provided the original author and source are credited.

a dynamically excited structural system for the suppression of its oscillatory motion is among the first passive vibration control strategies in the area of structural dynamics. In this context, Frahm [1] introduced the use of a linear spring-mass-damper device, the tuned mass damper (TMD) in 1909, to suppress excessive vibration in a variety of mechanical engineering applications [2–4]. Den-Hartog proposed an effective tuning approach [5], which has been extended by many researchers, e.g. Warburton [6]. An alternative connection arrangement was consequently proposed, termed the non-traditional TMD [7]. In contrast to the traditional TMD which has one point attached to the primary structure, such device has two attachment points, respectively connected to the reaction mass via a spring and a damper. More effective seismic-vibration mitigation performance has been demonstrated using this type of device [8].

More recently, by adding an inerter into the TMD and employing two structural attachment points, Marian and Giaralis [9] proposed a new vibration suppression device, the tuned mass damper inerter (TMDI). The inerter is a relatively new passive mechanical element, introduced by Smith [10], having the property that the generated force is proportional to the relative acceleration across its two terminals. Inerter-based absorbers have been shown to be effective in various applications, such as automotive [11], buildings [12–15] and railway vehicles [16–18]. For the TMDI, it has been shown in [9] that enhanced performance can be achieved compared with the TMD. It has also been shown in [19] that under some conditions, the TMDI outperforms the tuned inerter damper (TID [12]), which is equivalent to a TMDI with zero mass. The significant benefits of the TMDI demonstrate the potential advantages of mass-included vibration absorbers, with all three types of two-terminal mechanical elements (springs, dampers and inerters) included.

The existing mass-included dynamic absorbers have all been proposed using an ad hoc approach. However, when considering mass-included absorbers with springs, dampers and inerters, there are countless topological connection possibilities, some of which can potentially provide much more advantageous performance. An approach, to systematically cover a wide range of these connection possibilities, is yet to be developed. This paper establishes an approach to systematically characterise a full set of passive vibration absorbers with series-parallel¹ connections of one reaction mass and a pre-determined number of springs, dampers and inerters. Classical network synthesis (e.g. [20,21]) and graph theory (e.g. [22,23]) are used to facilitate the enumeration of topological connection possibilities. Using the proposed approach, the optimum reaction-mass absorber can be obtained for given vibration suppression problems.

This paper is structured as follows. In Section 2, vibration suppression of an example structure is studied using existing absorbers. In addition, the problem of identifying the optimum vibration absorber with one reaction mass including one or two attachment points is formulated. Section 3 enumerates all the possible mass-included absorber layouts with one attachment point, with which the optimum vibration absorber and the corresponding performance benefits are identified for the example structure. Section 4 proposes an approach to construct generic Immittance-Function-Networks – this captures the full set of absorber possibilities with two attachment points. In Section 5, the proposed approach for absorbers with two attachment points is applied to the example structure, illustrating the performance advantages that can be achieved. Conclusions are drawn in Section 6.

2. Existing approach and problem formulation

(a) Previous-studied absorbers applied to an example structure

Several passive absorbers, consisting of masses, springs and dampers, have been proposed for mitigating unwanted vibrations, the best known is the tuned mass damper (TMD [3]), see Figure 1(a). In the figure, 1 and 2 indicate two attachment points to the structure (or terminals in network synthesis terminology). As the TMD has a single attachment point, 2 is not connected. An

¹We use series, rather than serial, in this work as the more common usage when describing serial connections is series, e.g. [24].

alternative spring-damper-mass device, the non-traditional TMD [7] with two attachment points, has also been proposed, as shown in Figure 1(b). Popular examples of two terminal devices, that use an inerter rather than a mass, include the TID [12] and the L2 [25] shown in Figure 1(c, d). A third class of devices is one which uses both mass and inerter elements – an example is the TMDI [9], Figure 1(e).

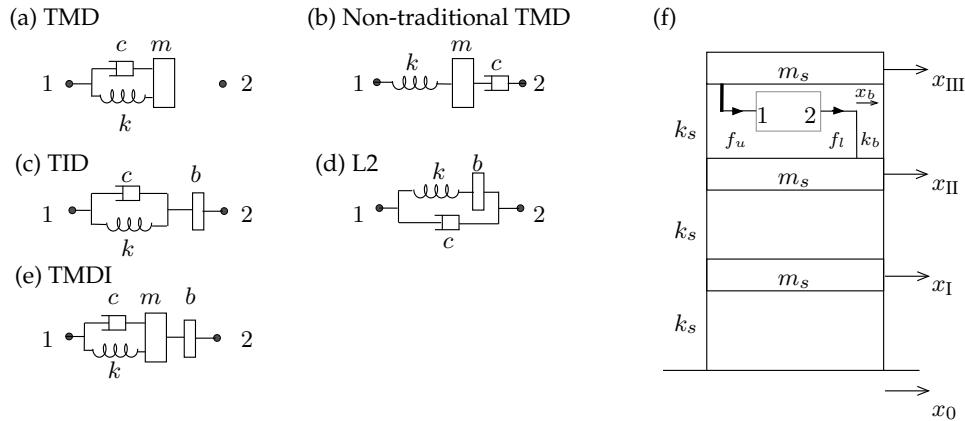


Figure 1: Schematic plot of example passive vibration absorbers (a) the TMD, (b) the non-traditional TMD, (c) the TID, (d) the L2 and (e) the TMDI, and a 3 DOF structure model (f).

In order to demonstrate the vibration suppression abilities of these and other devices, a three degree of freedom (DOF) structure model subjected to earthquake excitation, as shown in Figure 1(f), is introduced, with floor masses m_s and inter-storey stiffness k_s . The structural damping is taken to be zero as it is typically negligible compared with that introduced by absorbers. Note that the TID is more effective in vibration suppression when placed at the bottom of the building, while the TMD and the TMDI are more effective at the top. However, since the focus of this work is on the optimum mass-included vibration absorber identification methodology, we only consider the absorbers mounted at a single location, at the top of the building as shown in Figure 1(f). Here it exerts forces $-f_u$ and $-f_l$ on the upper and lower floors, respectively. The forces are defined as positive to the right on the absorber. Vibration suppressors attached to two floors are usually installed via a brace that spans between storey levels. Inevitably this brace has some compliance, so a brace stiffness k_b in series with the absorber and connecting to the lower floor is included. In this study, the structure parameters are adopted as $m_s = 10000$ kg, $k_s = 15000$ kN/m, and the brace stiffness is taken as $k_b = 0.2k_s$, in line with [26]. The equation of motion for the model of Figure 1(f), in matrix form, in the Laplace domain, can be derived as

$$\begin{bmatrix} m_s & 0 & 0 \\ 0 & m_s & 0 \\ 0 & 0 & m_s \end{bmatrix} s^2 \mathbf{X} + \begin{bmatrix} 2k_s & -k_s & 0 \\ -k_s & 2k_s & -k_s \\ 0 & -k_s & k_s \end{bmatrix} \mathbf{X} = \begin{bmatrix} k_s X_0 \\ -F_l \\ -F_u \end{bmatrix} \quad (2.1)$$

where in Laplace domain, $\mathbf{X}(s) = [X_I, X_{II}, X_{III}]^T$ represents the floor displacement vector, and $X_0(s)$ is the ground displacement (note $x_i(t) \xrightarrow{\mathcal{L}} X_i(s)$, $x_0(t) \xrightarrow{\mathcal{L}} X_0(s)$, and $f_u(t) \xrightarrow{\mathcal{L}} F_u(s)$, $f_l(t) \xrightarrow{\mathcal{L}} F_l(s)$). Due to the brace stiffness k_b , an additional DOF with displacement x_b is introduced, where $F_l = k_b(X_{II} - x_b)$ in the Laplace domain. In this example, the inter-storey drift displacement, which is a measure of the potential seismic damage of a structure, is taken as the performance measure. The frequency response function of i th floor inter-storey drift displacement, denoted as X_{d_i} , can be obtained from (2.1) with $X_{d_i} = X_i - X_{i-1}$, where $i = I, II, III$. The objective function, related to the inter-storey drift displacements, is then defined

as

$$J_d = \text{Max}_{(\text{over } i)} \left(\text{Max}_{(\text{over } \omega)} |T_{s^2 X_0 \rightarrow X_{d_i}}| \right), \quad (i = \text{I, II, III}), \quad (2.2)$$

where $T_{s^2 X_0 \rightarrow X_{d_i}}$ denotes the transfer function from the earthquake acceleration to the inter-storey drift displacements and $\text{Max}|T_{s^2 X_0 \rightarrow X_{d_i}}|$ is the maximum magnitude of $T_{s^2 X_0 \rightarrow X_{d_i}}$.

Consider the four example vibration suppressors shown in Figure 1(a-e). The value of the reaction mass in the vibration absorbers is selected as $m = 1000$ kg for the TMD and the TMDI, approximately 3.6% of the first modal mass. The optimisation is carried out to minimise the value of the objective function J_d . By selecting the component coefficients of each absorber layout, the optimum value of J_d is obtained and summarised in Table 1. Note that Matlab is used for the optimisation throughout this work, using the optimisation function *patternsearch* to obtain approximate optimum solutions, with the genetic algorithm ‘‘GPS basis 2N’’ [27]. The solutions from the *patternsearch* algorithm are then used as initial estimates for the gradient-based function *fminsearch* for fine-tuning. The convergence criterion for both *patternsearch* and *fminsearch* is a certain pre-determined tolerance on the change in the value of the cost function over the iteration. In this study, the relative tolerance is set to be 1×10^{-4} . Furthermore, to identify the global minimum, multiple starting points have been used for the *patternsearch* optimisation. From Table 1, it can be seen that the TMDI provides a 42% performance improvement over the TMD and also outperforms the TID, the L2 and the non-traditional TMD with 26%, 43% and 74% smaller values of J_d for this example structure and reaction mass. The frequency responses of the inter-storey drift displacements with the three devices, the TMD, TID and TMDI are shown in Figure 2, with short horizontal lines indicating the value of J_d . It can be noticed from this figure that the TMDI device results in the smallest drift displacements in the vicinity of all three structural modes of the 3 DOF structure. Note that the responses of the non-traditional TMD and the L2 absorbers are not shown in Figure 2 due to their large J_d values.

Table 1: Optimisation results for the example previous-studied layouts shown in Figure 1 with $m = 1000$ kg where applicable.

Configurations	Performance J_d ($\times 10^{-3} \text{ s}^2$)	Optimal parameter values (kg, kNs/m, kN/m)
TMD	25.0 (–)	$c = 11.6, k = 2.75 \times 10^2$
Non-traditional TMD	55.0 (-120%)	$c = 22.0, k = 1.81 \times 10^2$
TID	19.6 (21.6%)	$b = 7.94 \times 10^3, c = 7.50 \times 10^2, k = 4.35 \times 10^3$
L2	25.5 (-2.00%)	$b = 4.79 \times 10^3, c = 32.6, k = 3.53 \times 10^3$
TMDI	14.5 (42.0%)	$b = 1.12 \times 10^3, c = 9.50, k = 6.22 \times 10^2$

The significant performance benefit of the TMDI over the studied TMD and the inerter-based TID demonstrates the potential advantages of mass-included inerter-based absorbers where all four mechanical elements, inerters, dampers, springs and masses are used. The possible topological connections with these four types of elements are numerous. Hence, it is extremely challenging to systematically identify the most beneficial configurations amongst them. To this end, a systematic approach will be developed in this work.

(b) Problem formulation

Series-parallel mechanical networks with one reaction mass and any pre-determined number of inerters, dampers and springs are considered in this paper. For the two-terminal networks consisting only of non-mass elements, the network synthesis theory (e.g. [20,21]), developed in the electrical domain, has been adopted to facilitate a systematic analysis, making use of the force-current analogy [28]. Compared with electrical realisations, vibration absorbers have strict weight and space constraints for real-life implementations. Hence, it is crucial to minimise the required element number in the mechanical networks. This observation led to the structure-immittance approach [29] being proposed for devices consisting of inerters, dampers and springs.

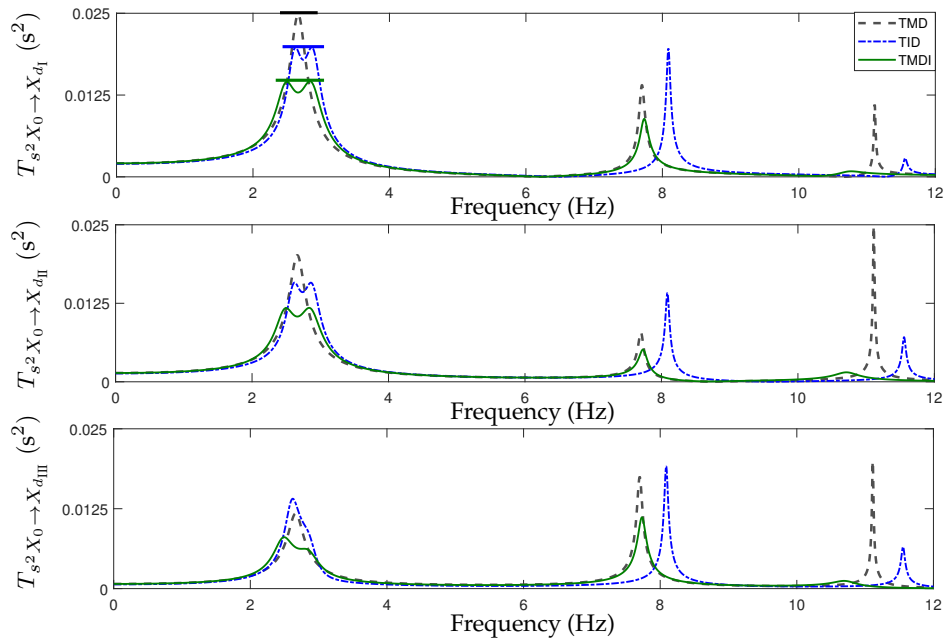


Figure 2: Frequency response in inter-storey drifts for the TMD (black dashed), TID (blue dash-dotted) and the TMDI (green solid).

This approach, which employed network synthesis theory, made use of the fact that all three of these element types have two terminals. When a reaction mass is included into the networks, a systematic approach becomes much more challenging, as the reaction mass is a one-terminal element (its centre of mass, Figure 3(a1)).

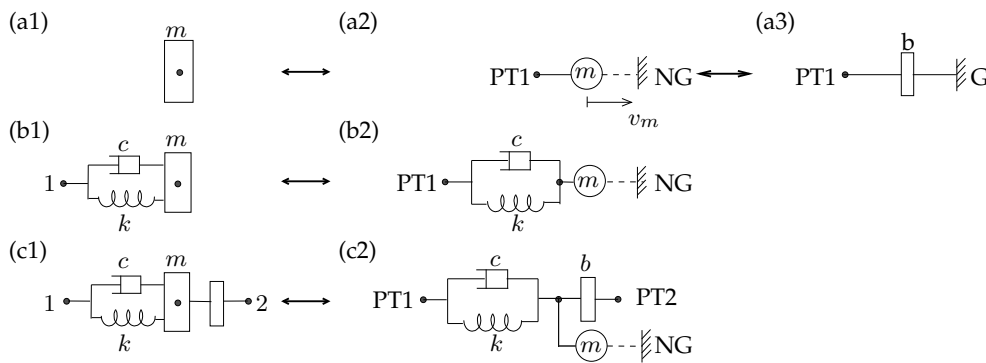


Figure 3: Absorber schematic plots and their network representations: (a1) a reaction mass with its network representation (a2), and (a3) an inerter with one terminal connected to ground (G); (b1) The TMD with its network representation (b2); (c1) the TMDI with its network representation (c2).

In order for network synthesis to be directly applicable to systematic enumeration of vibration absorbers with a reaction mass, it is necessary to treat the mass as a special two-terminal element, with one terminal notionally connected to the ground, denoted as a notional-ground (NG). Note it is not actually connected to ground, in contrast to an electrically grounded capacitor which is its equivalent in the force-current analogy [10]. The network representation of the mass is shown in Figure 3(a2), with the property that $F(s) = m(sV_m - 0)$, where V_m is the velocity of the mass with its value defined as positive to the right. Accordingly, in this work, terminals connected to physical attachments are denoted as physical-terminals (PTs) when considering their network representations. Note that mathematically a mass element is equivalent to an inerter with one of

the two terminals physically connected to ground, see Figure 3(a3). However, the mass element has its unique merit since attaching absorbers' terminals physically to the ground is unrealistic for a lot of applications. With the proposed network representation of the mass (Figure 3(a2)), the two mass-included suppression devices, the TMD and the TMDI (Figure 3(b1) and (c1)), can be depicted as networks, as shown in Figures 3(b2) and (c2). By denoting the absorber attachment points 1 (2) as PT1 (PT2) in the network representation, the TMD with one attachment point becomes a two-terminal network with one PT and one NG, termed a '1PT1NG network'. It can also be noted that for the TMDI device with two attachment points, its corresponding network, shown in Figure 3(c2), is no longer two-terminal, but a three-terminal network with two PTs and one NG, denoted as a '2PT1NG network'. Similarly, the non-mass absorbers with two attachment points, e.g. the TID (Figure 1(c)) are termed '2PT networks'. Note that the spring, damper and inerter elements can be regarded as special cases of 2PT networks, and are termed '2PT elements'.

Considering the fact that most vibration suppression devices have no more than two attachment points, our investigation focuses on 1PT1NG and 2PT1NG networks. The 1PT1NG network, represented by its force-velocity transfer function $H(s) = F_1(s)/V_1(s)$ is shown in Figure 4(a), where at the PT1, the force f_1 ($F_1(s)$ in the Laplace domain) is applied and results in a velocity v_1 ($V_1(s)$). Figure 4(b) shows a 2PT1NG network, with forces f_1, f_2 and velocities v_1, v_2 at two PTs. Note that because of the reaction mass, in contrast to the 2PT network (whose immittance function is $Y(s) = F(s)/(V_1(s) - V_2(s))$, see Figure 4(c)), the forces f_1, f_2 of the 2PT1NG network are not equal and opposite. To describe the relations between the velocities and the forces in the Laplace domain, an Immittance-Function-Matrix (IF-Matrix), denoted as $L(s)$, is required. The derivation of IF-Matrix for a given 2PT1NG network is detailed in Appendix A.

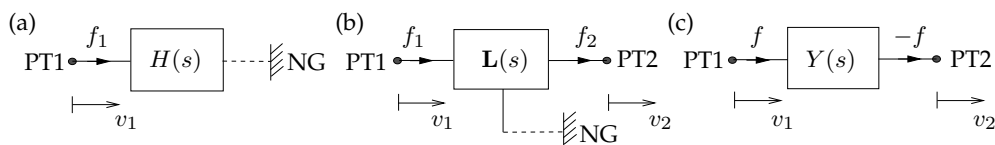


Figure 4: (a) 1PT1NG network, (b) 2PT1NG network and (c) 2PT network.

The rest of the paper addresses the following two questions:

- (1) Given one reaction mass and any pre-determined number of inerters, dampers and springs, how to enumerate all possible series-parallel '1PT1NG' and '2PT1NG' network layouts?
- (2) Based on (1), how to systematically identify the optimum absorber configuration for a given vibration suppression problem?

In order to address Question (1), procedures to construct 1PT1NG and 2PT1NG Immittance-Function-Networks (IF-Networks) need to be introduced. Here, an IF-Network refers to a network layout with its 2PT sub-networks represented by Immittance-Function-Blocks (IF-Block, e.g. Figure 4(c)). Generic IF-Networks which capture all IF-Network possibilities for given conditions will be identified. Different distribution cases of the pre-determined numbers of inerters, dampers and springs in the IF-Blocks of the generic IF-Networks will then be discussed, to obtain all possible series-parallel 1PT1NG and 2PT1NG network layouts. In the subsequent sections, the 1PT1NG networks will be firstly discussed, followed by the 2PT1NG cases. It turns out that the 2PT1NG case is much more complicated, but can provide significantly enhanced performance.

3. 1PT1NG network layout enumeration and case demonstration

This section considers the 1PT1NG network layouts with a reaction mass. The series and parallel connections between a 2PT network (represented by an IF-Block) and a 1PT1NG network are first described using concepts defined in graph theory [22]. A generic IF-network is then formulated, from which all possible 1PT1NG networks with a pre-determined number of 2PT elements can be

enumerated. Subsequently, a case study is demonstrated where the 2PT elements are specified as one inerter, one damper and one spring.

(a) Connection between 2PT and 1PT1NG networks

While connecting 2PT and 1PT1NG networks is relatively straightforward, we choose to introduce concepts defined in graph theory [22] to describe the process as they are necessary for the more complicated 2PT1NG network constructions later. In the electrical domain [30], a graph is used as a general representation of topological connections, consisting of a finite number of vertexes and branches. Here the correspondence between graphs and mechanical networks are introduced.

For a two-terminal mechanical network with specific connection topology, by depicting each element of the network as a branch, the two terminals and internal connection points as vertexes, the network can be represented as a graph, with a set of branches interconnected at their vertexes. For example, consider a network with only one mechanical element, such as the spring shown in Figure 5(a1), this can be represented as a graph with one branch, Figure 5(b1), where two vertexes shown as solid circles correspond to the two PTs, termed the terminal-vertexes. The graph of an example 2PT network, the TID of Figure 5(a2), is provided in Figure 5(b2). In this example, an intersection vertex exists, shown as a hollow circle, representing the inter-connected node of the TID. For a 1PT1NG network example, consider the TMD (Figure 5(a3)); its graph is shown in Figure 5(b3) with one terminal-vertex corresponds to a NG in the mechanical domain. In this way, all 2PT and 1PT1NG networks can be represented as a graph with two terminal-vertexes.

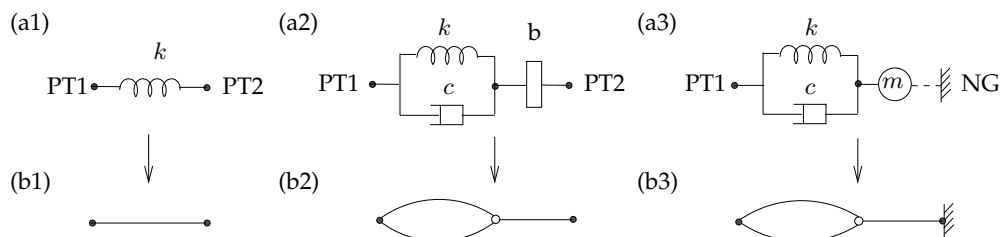


Figure 5: Example two-terminal mechanical networks and their corresponding graphs: (a1) a spring, (a2) the TID, (a3) the TMD and (b1), (b2), (b3) the corresponding graphs.

In [22], the series and parallel connections between graphs with two terminal-vertexes are defined. It states that the series connection is to coalesce one terminal-vertex of each graph into an intersection-vertex of the resulting two-terminal graph, of which the two terminal-vertexes are the remaining ones of the two connected graphs. Alternatively, a parallel connection is where two terminal-vertexes of each graph are connected together to formulate the two terminal-vertexes of the resulting two-terminal graph. Note that both these connection types can only be applied to terminal-vertexes. Based on this definition, we consider joining a 2PT network with a 1PT1NG network. Taking the graphs of Figure 6(a1) and (a2) as an example, we can note that only the series-connection is possible, as a parallel connection would necessitate a NG being connected with a PT. The series connection between these two graphs results in the graph shown in Figure 6(a3). As a graph is a general representation, each branch can represent different elements. Also there can be more branches between two vertexes and there can be more intersection vertexes in a graph. The three graphs, Figure 6(a1-a3), can correspond to the three general network representations shown in Figure 6(b1-b3), where $Y(s)$ is an IF-Block representing any possible series-parallel 2PT network and $H(s)$ is a 1PT1NG network. As an example by depicting the IF-Block $Y(s)$ as a spring (Figure 6(c1)) and the 1PT1NG network $H(s)$ as a TMD of Figure 6(c2), the series connection between them formulates the network shown in Figure 6(c3).

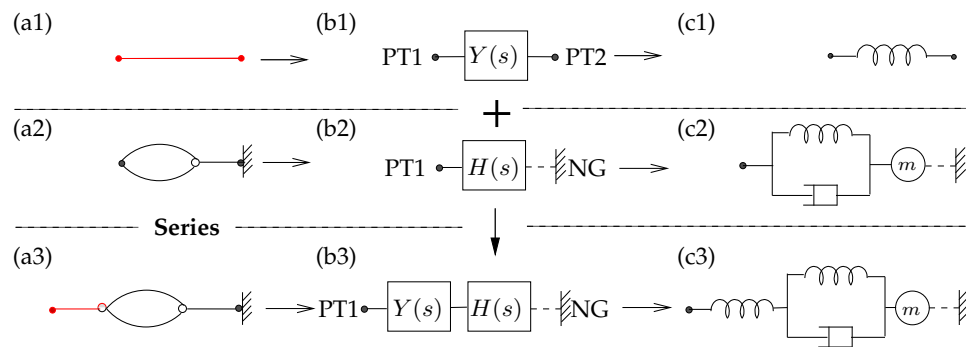


Figure 6: Example series connection between a 2PT network and a 1PT1NG network, represented as connections between (a) graphs, (b) IF-Networks and (c) example network layouts.

(b) Network layout enumeration using the generic 1PT1NG IF-Network

In order to formulate series-parallel 1PT1NG IF-Networks, a collection of a reaction mass and a finite number of IF-Blocks is now considered. A non-unique connection sequence is proposed, with which all possible 1PT1NG IF-Networks can be obtained. In the procedure, after each step, any obvious network simplification will be carried out. For example, if two IF-Blocks are connected in series or in parallel, they will be reduced to a single IF-Block. Start with a single IF-Block, it can be connected in series or in parallel with other IF-Blocks, however, these always reduce to a single IF-Block. At a certain step, the resulting IF-Block is connected to the mass, based on Figure 6, only a series connection is possible, resulting in a new 1PT1NG network. Further addition of IF-Blocks can only be connected in series with this 1PT1NG network, which can be reduced to a single IF-Block. Hence, all the IF-Networks can be represented by the generic IF-Network shown in Figure 7 with a single IF-Block $Y(s)$.

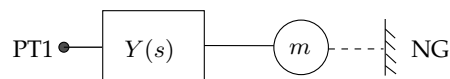


Figure 7: The generic 1PT1NG IF-Network.

Consider the 1PT1NG network layouts with one reaction mass and a pre-determined number, N , of 2PT elements. All the network possibilities can be obtained using the generic IF-Network of Figure 7, by enumerating the full class of 2PT network possibilities consisting of N elements in the IF-Block $Y(s)$. To this end, the structure-immittance approach [29], developed to systematically express all possible series-parallel networks with pre-determined number of 2PT elements, can be directly applied. The obtained structural immittance $Y(s)$ is then used to express the transfer function of the generic IF-Network, see Figure 7, as:

$$H(s) = Y(s)ms / (ms + Y(s)) \quad (3.1)$$

With this transfer function, the optimum 1PT1NG vibration absorber with a reaction mass can be identified for a given vibration suppression problem.

(c) 1PT1NG network case demonstration

To illustrate the enumeration and the systematic identification approach, a 1PT1NG case with one reaction mass, one damper, one spring and one inerter is analysed. From the generic IF-Network of Figure 7, in total 8 network layouts can be enumerated by allocating all possible series-parallel 2PT networks consisting of one each of the three 2PT element types (see Table 2 in [29]), into the IF-Block. The immittance function $Y(s)$ is then formulated using the structure-immittance

approach to cover all 2PT network possibilities, given by [29]:

$$Y(s) = \frac{bcs^2 + b(k_4 + k_6)s + c(k_2 + k_6)}{bc(1/k_3)s^3 + bs^2 + cs + k_2 + k_4}, \quad (3.2)$$

or

$$Y(s) = \frac{bc(1/k_1 + 1/k_2)s^3 + bs^2 + cs + k_3}{b(1/k_1 + 1/k_5)s^3 + c(1/k_2 + 1/k_5)s^2 + s} \quad (3.3)$$

with the condition that $b \geq 0$, $c \geq 0$, $k_i \geq 0$, and for the function (3.2), at least three of the parameters $k_2, 1/k_3, k_4, k_6$ must equal zero (covering four 2PT networks), and for (3.3), at least three of the parameters $1/k_1, 1/k_2, k_3, 1/k_5$ must equal zero (covering the other four 2PT networks). The transfer function of the generic IF-Network, $H(s)$ of (3.1), with $Y(s)$ expressed as (3.2) or (3.3) can now be used for the optimum absorber identification.

The 3 DOF structure shown in Figure 1(f) is taken as an application example. The 1PT1NG network layouts consisting of one reaction mass (1000 kg as before), one inerter, one damper and one spring, connected to the top storey of the structure, are considered as candidate absorber layouts. By optimising the objective function (2.2) with the transfer function $H(s)$

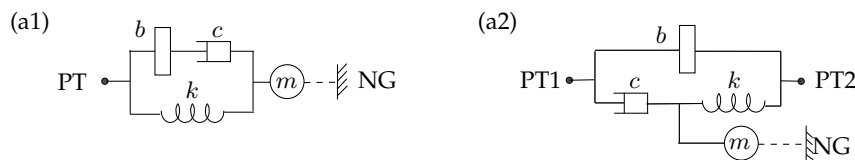


Figure 8: (a1) The optimum 1PT1NG configuration C1 and (a2) a 2PT1NG network example C2.

(3.1), the optimum absorber configuration, C1, is shown in Figure 8(a1), with the corresponding parameter values obtained as $b = 1.05 \times 10^3$ kg, $c = 30.5$ kNs/m, $k = 4.92 \times 10^2$ kN/m. With this configuration, the optimum result of the objective function is $J_d = 0.016$, providing a 35% and a 17% performance improvement compared with the TMD and the TID, respectively. However, when compared to the 2PT1NG network, the TMDI, it can be seen from Table 1 that the optimal 1PT1NG configuration, C1, is unable to match its vibration suppression performance, resulting in a 11% larger value of J_d . In addition to the TMDI, there are numerous other 2PT1NG networks that use the same numbers of each type of element, for which even higher performance benefit might be achievable. For example, the mass-included absorber (termed C2) shown in Figure 8(a2) is a 2PT1NG network, with which the objective function J_d can be reduced to 0.014 with $b = 1.21 \times 10^4$ kg, $c = 13.9$ kNs/m and $k = 2.98 \times 10^2$ kN/m. It can be seen that the C2 outperforms the TMDI by 6.7%. The inter-storey drift frequency responses of the structure model with all five proposed absorbers are shown in Figure 9. These results motivate the following investigation into the full class of 2PT1NG networks made up of one reaction mass and a pre-determined number of inerters, dampers and springs.

4. 2PT1NG network layout enumeration

In this section, 2PT1NG network layouts with a reaction mass are considered. The series and parallel connections between a 2PT and a 2PT1NG network are firstly described, after which a procedure for formulating 2PT1NG IF-Networks is introduced. The generic 2PT1NG IF-Networks, covering all the IF-Network possibilities with a given number of IF-Blocks, are formulated. Using these generic IF-Networks, the enumeration of all possible network layouts is then discussed, together with the IF-Matrix derived for systematic optimisation.

(a) Connection between 2PT and 2PT1NG networks

Using the same correspondence between mechanical networks and graphs, as used in Section 3(a), any 2PT1NG network can be represented by a three-terminal graph with one of the terminal-vertices corresponding to the NG. Taken the TMDI (Figure 10(a1)) as an example, its graph

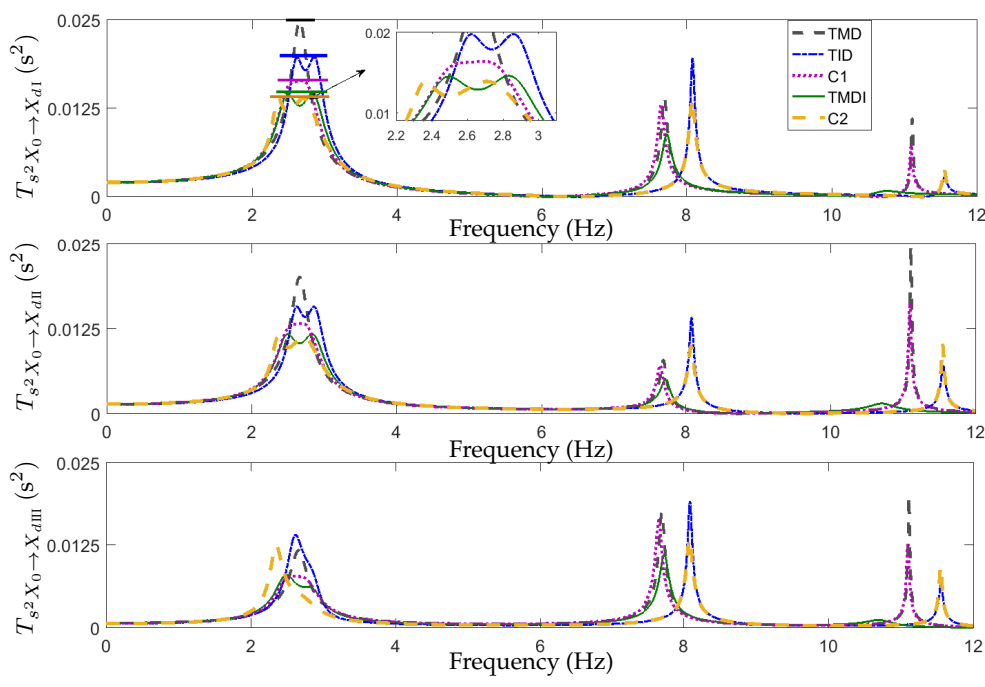


Figure 9: Frequency response in inter-storey drifts with the TMD (black dashed), TID (blue dash-dotted), the TMDI (green solid), the C1 (purple dotted) and the C2 (thick orange dashed).

representation can be depicted as Figure 10(a2), which consists of three terminal-vertexes and one intersection-vertex.

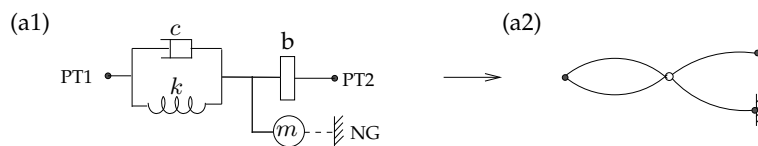


Figure 10: An example 2PT1NG network, the TMDI, (a1) and its graph representation (a2).

To formulate the series-parallel 2PT1NG networks, the series and parallel connections between a 2PT and a 2PT1NG network also need to be introduced based on the definitions for three-terminal graphs [23]. In [23], the series connection concept is similar to that for the connection between two two-terminal graphs, described in the previous section. For a parallel connection, both terminal-vertexes of a two-terminal graph and two of the three terminal-vertexes of a three-terminal graph are connected together. The resulting graph has three terminal-vertexes of the original three-terminal graph but now two of these are shared with the original two-terminal graph. Based on these observations, considering the connection of an example two-terminal graph corresponding to any 2PT network (Figure 11(a1)) and a three-terminal graph shown in Figure 11(a2) representing a 2PT1NG network, the series connection results in the two possibilities, shown in Figure 11(a3) and (a4), respectively. By coalescing one terminal-vertex of Figure 11(a1) with the left terminal-vertex of Figure 11(a2), Figure 11(a3) is obtained, while Figure 11(a4) is formulated by connecting Figure 11(a1) with the right terminal of Figure 11(a2). Figure 11(a5) shows the graph obtained by the parallel connection; because of the existence of NG, the parallel connection can only result in this possibility. The general network examples obtained from the graphs are shown in Figure 11(b1-b5). By depicting the general network representations $Y(s)$ and $L(s)$ as specific layout examples, the series and parallel connections between a 2PT network (spring) and a 2PT1NG network (TMDI) are shown in Figure 11(c1-c5).

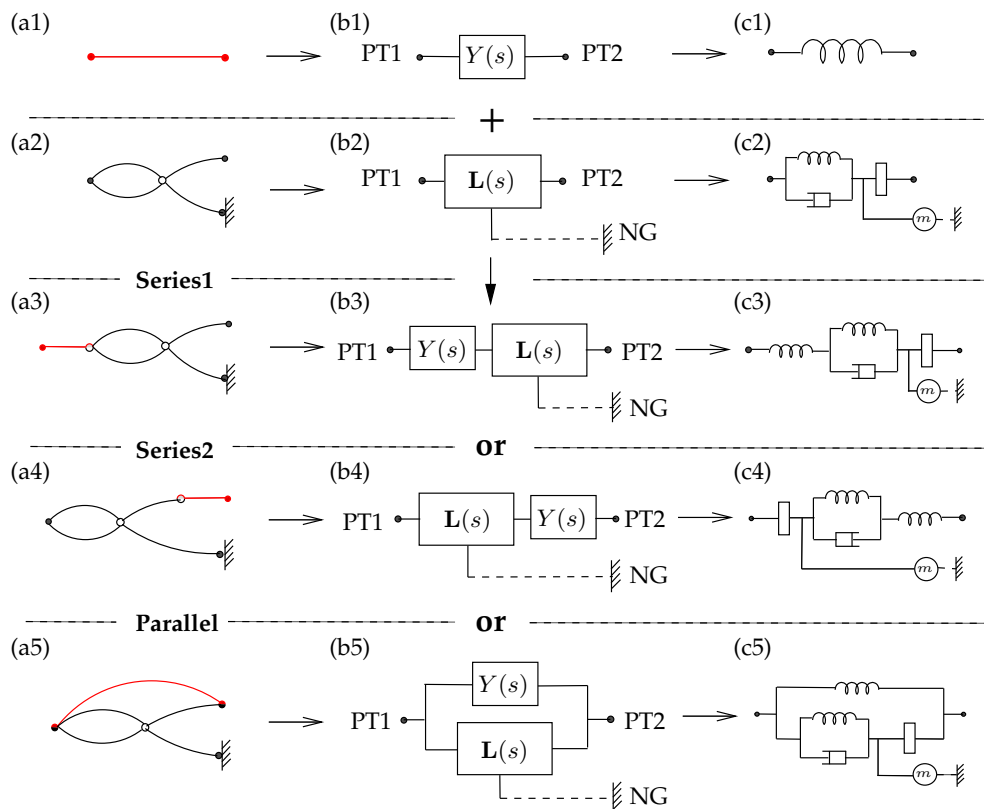


Figure 11: Example series and parallel connection between a 2PT network and a 2PT1NG network, represented as connections between (a) graphs, (b) IF-Networks and (c) example network layouts.

(b) Formulation of generic 2PT1NG Immittance-Function-Network

In order to formulate 2PT1NG IF-Networks, similar to 1PT1NG case, a collection of a reaction mass and a finite number of IF-Blocks is now considered. A sequence of steps is introduced based on the work of Nishizeki & Saito [23], shown in Figure 12. At each step, a sub-network (either a 1PT1NG network or an IF-Block) is connected in series or in parallel with the network formed in the previous step. While such procedure is not unique, using this procedure, any series-parallel 2PT1NG IF-Network which can be formed from the original set can be obtained. In the procedure, after each formulation step, we will carry out any obvious network simplification, same as the simplifications we carried out for the 1PT1NG case, for example if two IF-Blocks are connected in series or in parallel, they will be reduced again to a single IF-Block. Similar to [23], in which the construction of a three-terminal series-parallel graph begins with an empty graph, Figure 12–Step 1 is taken as the start. We first consider joining the two terminals, PT1 and NG. Using the generic 1PT1NG IF-Network obtained in Section 3(b) (Figure 7), a new network shown in Figure 12–Step 2 is obtained. The next step is to add a single IF-Block $Y_2(s)$ to the network, resulting in Figure 12–Step 3 (via a parallel connection between the terminals PT1 and PT2). Consider adding the next IF-Block, $Y_3(s)$, resulting in the new IF-Network shown in Figure 12–Step 4 using the Series1 connection in Figure 11. Note that all the other connection possibilities between Figure 12–Step 3 and the IF-Block $Y_3(s)$ can all be simplified to Figure 12–Step 3. At this point, only a parallel IF-Block can be added, with the resulting IF-Network shown in Figure 12–Step 5, since series IF-Blocks can be reduced to the network of Step 4. Following this parallel addition, only series additions modify the network. Both Series1 and Series2 connections in Figure 11 need to be considered, and we define connecting to PT2 as Step 6, resulting in the network of Figure 12–Step 6. An additional IF-Block is then added in series at PT1 – the resultant network is shown in

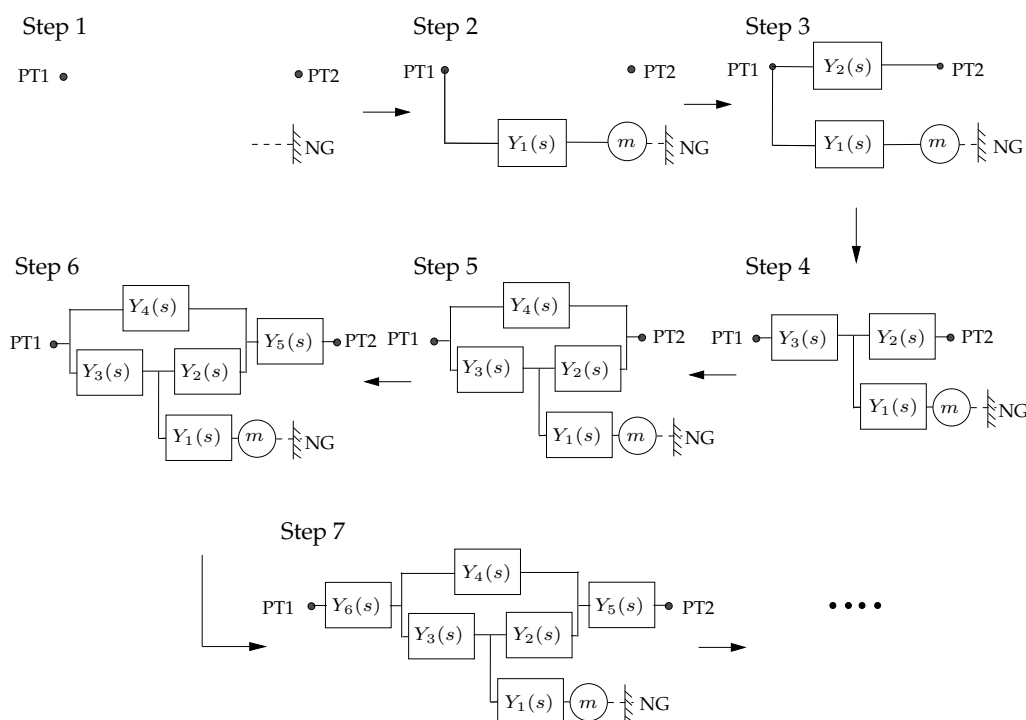


Figure 12: A procedure to form all possible series-parallel 2PT1NG IF-Networks with a reaction mass and a pre-determined number of IF-Blocks.

Figure 12–Step 7. Consequent steps will be adding IF-Blocks in parallel then in series by repeating Steps 5–7, until all IF-Blocks in the original collection are used. Following this procedure, all possible IF-Networks can be obtained.

In order to formulate generic IF-Networks, whether a specific IF-Block exists need to be discussed. To this end, the terminology *removed* and *present* are introduced here. An IF-Block is defined to be *removed* as its immittance function takes the value of 0 or ∞ — the value is chosen to ensure that the included components (i.e. the IF-Blocks and the reaction mass) or any two of the terminals, PT1, PT2 and NG, are not locked rigid and that none of the terminals is disconnected. An IF-Block is regarded as *present* if it is not removed. Consider the IF-Block $Y_1(s)$ shown in Figure 12; if it is removed, its immittance function must take the value of ∞ ; otherwise the NG will be disconnected. For $Y_2(s)$, its removal must correspond to $Y_2(s) = \infty$; otherwise the PT2 will be disconnected. Also for $Y_3(s)$, we must set $Y_3(s) = \infty$; otherwise the PT1 in Figure 12–Step 4 will be disconnected. Consider the parallel added IF-Block $Y_4(s)$: if it is removed, it must take the value of 0 (otherwise PT1 and PT2 in Figure 12–Step 5 will be locked rigid). For the series added IF-Blocks $Y_5(s)$ and $Y_6(s)$: we must set them as ∞ to ensure that the terminals of the resulting networks (see Figure 12–Step 6 and Step 7) are not disconnected. Following the same argument, the additional IF-Blocks added in parallel (series) connection must take the value of 0 (∞) when they are removed.

The rest part of this subsection focuses on generating generic IF-Networks. Different from 1PT1NG networks, where one generic IF-Network is sufficient (Figure 7), for 2PT1NG networks, different generic IF-Networks are needed depending on the number of IF-Blocks which are present. Now consider the possible 2PT1NG IF-Networks with a pre-determined number, R , of IF-Blocks. Suppose that the generic IF-Network, representing $R - 1$ IF-Blocks, has been formulated, denoted as $L_{R-1}(s)$, all the IF-Networks with R IF-Blocks can be subsequently obtained by adding an extra IF-Block to it. The generic IF-Network, $L_R(s)$, covering all the obtained IF-Network possibilities, can then be formulated, satisfying the condition that R IF-Blocks are present. Following this argument, the generic IF-Network for any R value can be formulated.

Note that the generic IF-Network has more IF-Blocks than is allowed, hence requires the condition that R IF-Blocks are present. We will now discuss the $R = 1$ case, then move on to $R = 2$ and beyond.

- For $R = 1$: We first consider the case where in Step 1 of Figure 12, $Y_1(s)$ is present. The resulting network is Figure 12–Step 2, which is a 1PT1NG network (with PT2 disconnected). Hence this case is not valid and $Y_1(s)$ must be removed. When $Y_2(s)$ is present, a 2PT1NG IF-Network is obtained, shown in Appendix B, Figure 15(a). If $Y_2(s)$ is not present, the connection of $Y_3(s)$ results in a new 2PT1NG IF-Network, see Figure 15(b), Appendix B. If $Y_3(s)$ is removed, PT1 and PT2 are rigidly connected and any follow on steps in Figure 12 only result in a 1PT1NG network. Hence, two network possibilities (Figure 15, Appendix B) are obtained for the $R = 1$ case, with which the generic IF-Network can be obtained as $\mathbf{L}_1(s)$ in Table 2, satisfying the condition that only one IF-Block is present.
- For $R = 2$: The IF-Networks can be formulated by adding one additional IF-Block to the generic IF-Network $\mathbf{L}_1(s)$ in Table 2. Firstly, we set both $Y_2(s)$ and $Y_3(s)$ in $\mathbf{L}_1(s)$ as present, this results in an IF-Network shown in Figure 16(a), Appendix B. We then consider the case where $Y_1(s)$ is present. This means either $Y_2(s)$ or $Y_3(s)$ can be present, resulting in two new IF-Networks shown in Appendix B, Figure 16(b, c). At last, an extra IF-Block $Y_4(s)$ is added to $\mathbf{L}_1(s)$ in parallel connection, and its present will result in the removal of $Y_2(s)$ or $Y_3(s)$, however, the resulting networks can be simplified to the network with one IF-Block. Hence, the network $\mathbf{L}_2(s)$ shown in Table 2 is the generic IF-Network for $R = 2$ case, satisfying the condition that two IF-Blocks are present.
- For $R = 3$: An extra IF-Block is added to the generic IF-Network $\mathbf{L}_2(s)$ in series or in parallel, to formulate all the IF-Networks with three IF-Blocks. We first set three IF-Blocks in $\mathbf{L}_2(s)$ as present, an IF-Network shown in Appendix B, Figure 17(a) is hence obtained. By adding an additional IF-Block $Y_4(s)$ in parallel to $\mathbf{L}_2(s)$, its present will result in the removal of $Y_1(s)$; otherwise the resulting network will be reduced to a network with two IF-Blocks. This results in an IF-Network of Figure 17(b). Hence, the generic IF-Network for $R = 3$ can be formulated as $\mathbf{L}_3(s)$ in Table 2, subject to the condition that three IF-Blocks are present.
- For $R = 4$: An IF-Network shown in Figure 18(a), Appendix B can be firstly obtained by setting all four IF-Blocks in $\mathbf{L}_3(s)$ as present. An extra IF-Block, $Y_5(s)$ is then added in series to the right of $\mathbf{L}_3(s)$ and if it is present, only the removal of $Y_1(s)$ can result in a new IF-Block, see Appendix B, Figure 18(b). Consider the case that $Y_6(s)$ is added in series to the left of $\mathbf{L}_3(s)$. An IF-Network of Figure 18(c) can be obtained. Hence, the generic IF-Network for $R = 4$ can be formulated as $\mathbf{L}_4(s)$ in Table 2, with the condition that four IF-Blocks are present.
- Generalisation: Using the similar argument, the generic IF-Network representing more numbers of IF-Blocks can be obtained, as shown in Table 2. For the odd R (with $R \geq 5$), the generic IF-Network is formulated by adding an IF-Block $Y_{\frac{3R-1}{2}}(s)$ in parallel to $\mathbf{L}_{R-1}(s)$. The subscript $\frac{3R-1}{2}$ of the IF-Block represents the total number of IF-Blocks required in the generic IF-Network, $\mathbf{L}_R(s)$. Also for the even R (with $R \geq 6$), the generic IF-Network can be formulated by series connecting two IF-Blocks $Y_{\frac{3R}{2}-1}(s)$ and $Y_{\frac{3R}{2}}(s)$ with $\mathbf{L}_{R-1}(s)$, where in total $\frac{3R}{2}$ numbers of IF-Blocks are required.

The generic IF-Network results of the above are summarised in Table 2, which can then be used for enumerating all possible network layouts.

Table 2: Generic 2PT1NG IF-Networks, $\mathbf{L}_R(s)$, with the condition of R IF-Blocks present

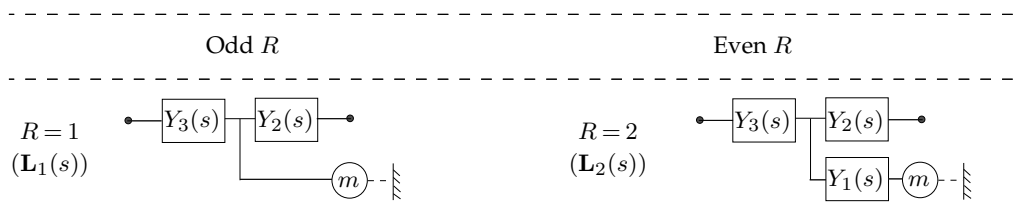
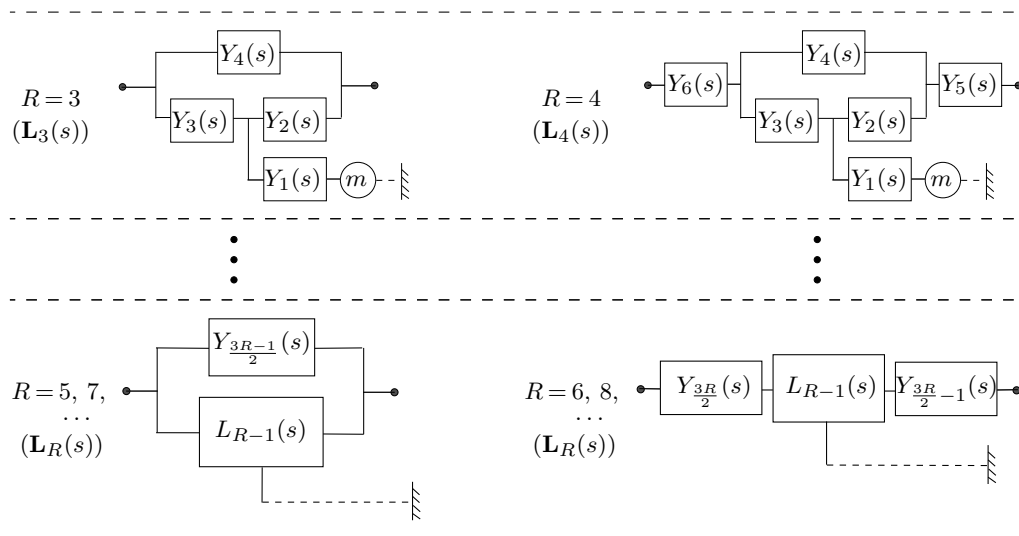


Table 2. (Continued)



(c) Network layout enumeration and Immittance-Function-Matrix derivation

For the enumeration of 2PT1NG network layouts with a reaction mass element and N 2PT elements (springs, dampers and inerters), the obtained generic IF-Networks with $R = 1, 2, \dots, N$ in Table 2 can be used. We first distribute the N 2PT elements into R present IF-Blocks (other IF-Blocks are removed), and secondly allocating element types into each present IF-Block. After this, the element types and numbers will be determined for each IF-Block in the generic IF-Networks. The structure-immittance approach [29] is then adopted to derive the corresponding immittance functions of the blocks, which is able to cover the full set of possible 2PT network connections.

With the obtained immittance functions of the included IF-Blocks, the IF-Matrix for each generic IF-Network is derived based on the procedure shown in Appendix A, which can then be used for optimisation studies. We denote that the IF-Matrix for a 2PT1NG network can be derived by deriving its equations of motion. However, there are a great number of possible network layouts, a more straightforward and simpler approach for deriving the IF-Matrix is needed – this is provided and explained in detail in Appendix A.

5. 2PT1NG network case demonstration

In this section, the 2PT1NG network case with one damper, one spring and one inverter is analysed. All the possible 2PT1NG network layouts are enumerated using the generic IF-Networks in Table 2. The IF-Matrix for each generic IF-Network is derived and applied to the example structure. Significant performance advantages with 2PT1NG network layouts will be demonstrated at the end of this section.

(a) Network layouts enumeration

For the 2PT1NG networks with one damper, one spring and one inverter, we have $N = 3$. Hence, three generic IF-Networks with $R = 1, R = 2$ and $R = 3$, shown as $\mathbf{L}_1(s)$, $\mathbf{L}_2(s)$ and $\mathbf{L}_3(s)$ in Table 2, will be used.

Consider the generic IF-Network for $R = 1$, $\mathbf{L}_1(s)$ of Table 2, all the three 2PT elements should be distributed in one IF-Block and the other IF-Block is removed. As a result, in total 16 2PT1NG network layouts are enumerated and for systematically analyse all of them, the structure-immittance approach [29] is adopted to express the immittance function of the present

IF-Block. The immittance function is the structural immittances for one inerter, one damper and one spring case, shown in (3.2) and (3.3). By expressing the force-velocity transfer function matrix of the generic IF-Network shown in Table 2 and making use of the condition that one IF-Block is removed, we can obtain the IF-Matrix $\mathbf{L}_1(s)$ as (A.3) in Appendix A, with the condition that one of the immittance functions, $Y_1(s)$, $Y_2(s)$, takes the expression as structural immittances of (3.2) and (3.3), and the other one must equal ∞ .

For the generic IF-Network with $R = 2$, shown as $\mathbf{L}_2(s)$ of Table 2, two of the three IF-Blocks are present, between which the three 2PT elements are distributed in. For these two present IF-Blocks, one should include one 2PT element and the other one consists of the remaining two elements. For example, when $Y_1(s)$ and $Y_2(s)$ in $\mathbf{L}_2(s)$ (Table 2) are present and $Y_1(s)$ includes one element, such as a spring, the other two elements (the damper and inerter) are contained in $Y_2(s)$, resulting in two network possibilities by connecting damper in series or in parallel with the inerter. Consider that there are three different element types and switching $Y_1(s)$ with $Y_2(s)$ will result in different network possibilities, the generic IF-Network with one IF-Block removed covers 36 network layouts. Finally, the IF-Matrix for this generic IF-Network, $\mathbf{L}_2(s)$, can be derived as (A.4) in Appendix A, where one of immittance functions $Y_1(s)$, $Y_2(s)$, $Y_3(s)$ equals ∞ , one is the force-velocity transfer function of a single 2PT element, and the third requests structural immittance for the remaining two 2PT elements. Consider the case that $Y_1(s)$ represents a spring k and $Y_2(s)$ includes one damper c and one inerter b , we should make $Y_3(s) = \infty$, $Y_1(s) = k/s$ and $Y_2(s)$ takes the expression of a structural immittance obtained for one damper and one inerter case, given as:

$$Y_2(s) = c_2(bs + c_1)/(bs + c_1 + c_2) \quad (5.1)$$

with the condition that one of the parameters c_1 or $1/c_2$ is positive and the other one equals zero.

Considering the generic IF-Network obtained for $R = 3$ case, shown as $\mathbf{L}_3(s)$ of Table 2, three of the four IF-Blocks must be present and each of them contains one 2PT element. By removing one IF-Block and distributing three different element types into the present IF-Blocks, all the 2PT1NG network layouts for this case can be enumerated. Note that when $Y_2(s)$ or $Y_3(s)$ is removed with its immittance function as ∞ , the resulting IF-Network will be reduced to that with two IF-Blocks, hence are omitted for the network layouts enumeration. From the generic IF-Network, in total 12 network layouts can finally be enumerated. These network layouts can be represented by the IF-Matrix $\mathbf{L}_3(s)$, derived based on (A.4) and (A.6) in Appendix A, given as

$$\mathbf{L}_3(s) = \left(\mathbf{L}_2(s) + Y_4(s) \begin{bmatrix} 1 & -1 \\ -1 & 1 \end{bmatrix} \right) \quad (5.2)$$

where either $Y_1(s) = \infty$ or $Y_4(s) = 0$ and the remaining three immittance functions are the force-velocity transfer functions of three different 2PT element types.

These obtained IF-Matrices can then be used for given vibration suppression problems. Importantly, using the method proposed here, all possible series-parallel 2PT1NG network layouts, with one reaction mass, one spring, one damper and one inerter are covered. In addition, by making use of the structure-immittance approach, all the possible layouts can be analysed in a systematic way and by optimising these using the objective functions considered, the optimal configuration can be obtained across all the network possibilities. In the following subsection, the results obtained in this part will be applied to the 3 DOF structure example, to illustrate the benefits of the proposed design approach. For the one reaction mass, one inerter, one damper and one spring case considered, in total 64 2PT1NG network layouts can be enumerated and covered by three generic IF-Networks, amongst which the optimum configuration can be obtained by three optimisations.

(b) Numerical application on the example structure

Consider the 3 DOF structure shown in Figure 1(f). The suppression system is taken to be the 2PT1NG network including one reaction mass, one inerter, one damper and one spring. The value

of the reaction mass is taken as 1000 kg, as the same as that used in previous two application examples (see Figure 2 and Figure 9).

For the 2PT1NG network with each of the four element types, three generic IF-Networks, $L_1(s)$, $L_2(s)$ and $L_3(s)$, are formulated in Section 5(a), covering all the 2PT1NG network possibilities. These obtained generic IF-Networks, together with their corresponding IF-Matrices (A.3, A.4, 5.2), are then used to minimise the objective function J_d . For example, for the 2PT1NG networks covered by the generic IF-Network, $L_1(s)$, the IF-Matrix (A.3) is adopted as the transfer function matrix of the vibration suppression device, with which the objective function J_d can be obtained based on (2.1, 2.2). In (A.3), the present immittance function $Y_2(s)$ or $Y_3(s)$ formulated using the structure-immittance approach is then optimised to identify the optimal 2PT network configuration out of all the eight possible layouts made up of one inerter, one damper and one spring (see Table 2 in [29]). Together with this obtained 2PT network, the optimal 2PT1NG

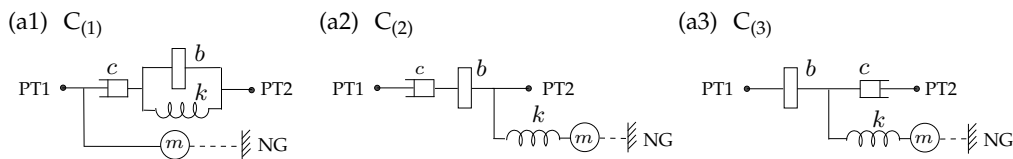


Figure 13: Optimal 2PT1NG configurations for the one inerter, one damper and one spring case for (a1) $R = 1$, (a2) $R = 2$ and (a3) $R = 3$ case.

network configuration can then be obtained from the corresponding generic IF-Network, $L_1(s)$, of Table 2. The optimal structures for three generic IF-Network cases with $R = 1, 2, 3$ have been obtained as Figure 13 (a1), (a2) and (a3), respectively. The corresponding optimal results in value of the objective function J_d (2.2) are summarised in Table 3, together with the optimum parameter values. The previously proposed layouts, such as the TMD, the TID, the TMDI, the C1 identified for the 1PT1NG networks (see Figure 8(a1)) and the C2 (see Figure 8(a2)) are also provided in Table 3 for a sake of comparison.

Table 3: Optimisation results for the one reaction mass, one inerter, one damper and one spring case.

Configurations	Performance J_d ($\times 10^{-3} \text{ s}^2$)	Optimal parameter values (kg, kNs/m, kN/m)
TMD (no b)	25.0 (-)	$c = 11.7, k = 2.75 \times 10^2$
TID (no m)	19.6 (21.6%)	$b = 7.94 \times 10^3, c = 7.50 \times 10^2, k = 4.35 \times 10^3$
C1 (a 1PT1NG device)	16.3 (34.8%)	$b = 1.05 \times 10^3, c = 30.5, k = 4.92 \times 10^2$
TMDI (a $R = 2$ case device)	14.5 (42.0%)	$b = 1.12 \times 10^3, c = 9.50, k = 6.22 \times 10^2$
C2 (a $R = 3$ case device)	13.8 (44.8%)	$b = 1.21 \times 10^4, c = 13.9, k = 2.98 \times 10^2$
$C_{(1)}$	19.5 (22.0%)	$b = 8.95 \times 10^3, c = 7.65 \times 10^2, k = 16.8$
$C_{(2)}$	10.2 (59.2%)	$b = 9.91 \times 10^3, c = 4.28 \times 10^2, k = 2.26 \times 10^2$
$C_{(3)}$	8.60 (65.6%)	$b = 8.10 \times 10^3, c = 3.26 \times 10^2, k = 2.13 \times 10^2$

For the generic IF-Network, $L_1(s)$ of Table 2, out of the 16 possible layouts, the optimisation indicates that the configuration $C_{(1)}$ is optimal. The corresponding optimal value of the objective function J_d is 0.0195 shown in Table 3, slightly smaller than that of the TID. Considering generic IF-Network representing two IF-Blocks, we notice that the TMDI is covered by this network ($L_2(s)$ of Table 2), with $Y_1(s) = \infty$, $Y_2(s) = bs$ and $Y_3(s) = k/s + c$. However, the TMDI is not the optimum configuration for this case, and the resulting optimum configuration is shown in Figure 13(a2), with which the value of J_d is obtained as 0.0102. It can be seen that comparing with the TMDI, $C_{(2)}$ can provide almost 30% performance improvement when $b = 9.91 \times 10^3 \text{ kg}$, $c = 4.28 \times 10^2 \text{ kNs/m}$ and $k = 2.26 \times 10^2 \text{ kN/m}$. Figure 13(a3) shows the

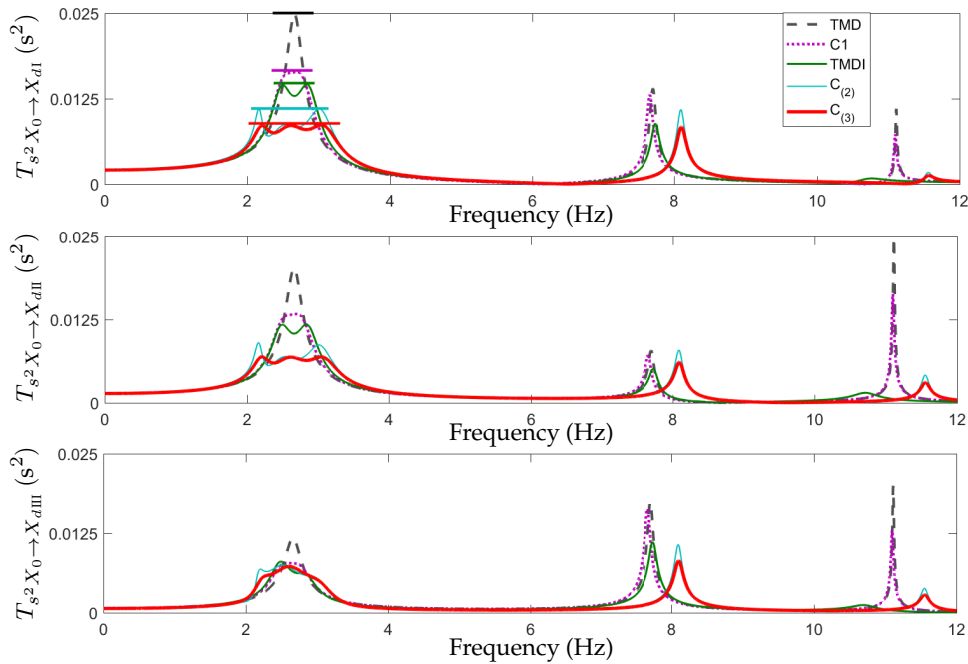


Figure 14: Frequency response in inter-storey drifts with the TMD (black dashed), the TMDI (green solid), the C1 (purple dotted), the $C_{(2)}$ (thin cyan solid) and the $C_{(3)}$ (thick red solid).

optimum absorber configuration $C_{(3)}$ for the $R = 3$ case, which gives the value of J_d as 0.0086, approximately 41% smaller than that of the TMDI and almost 66% better than the TMD. Also note that C_2 , Figure 8(a2) is a network layout included in the $R = 3$ generic IF-Network, however, the $C_{(3)}$ outperforms it, achieving a 38% smaller value of J_d . It can also be seen that the $C_{(3)}$ is the most effective vibration suppression device, amongst all the 64 series-parallel 2PT1NG networks consisting of one reaction mass and each of the three 2PT element types. From Table 3, we note that the configuration $C_{(3)}$ outperforms the C1 with 47% performance improvement in J_d . This suggests that the 2PT1NG network, i.e. one which has connection points on the second and third storey, can provide better seismic performance than the 1PT1NG one (which is connected to the third storey only) with the same numbers of each element type.

Figure 14 shows the frequency responses of the three inter-storey drifts of the structure model with the identified beneficial absorber configurations, subjected to the earthquake excitation. It can be seen that rather than splitting the first fundamental frequency into two separate frequencies, both the $C_{(2)}$ and the $C_{(3)}$ split it into three frequencies, hence resulting in smaller values of the drift displacements comparing with the other configurations, such as the TMDI. This is because both $C_{(2)}$ and $C_{(3)}$ contain additional DOF compared to the other devices. Also note that the configuration $C_{(3)}$ results in the smallest inter-storey drift values of all the three floors in the vicinity of not only the first fundamental frequency, but also the second and third fundamental frequencies.

6. Conclusion

This paper presents a systematic characterisation and analysis of passive vibration suppression devices with a reaction mass. Devices with one and two structural attachment points were considered, for which a full set of network layouts with pre-determined numbers of inerters, dampers and springs were captured and enumerated. This is achieved using generic IF-Networks to represent the topological connection possibilities of the mass and the IF-Blocks, and the structural immittances to describe the 2PT networks in each IF-Block. By using the force-velocity Immittance-Function-Matrices, the dynamics of vibration suppression devices with two

attachment points can be described and used for vibration suppression problems. A 3 DOF structure model under earthquake excitation is considered, and the number of inerter, damper and spring was restricted to be one for vibration suppression devices. Optimal configurations were obtained out of 16 and 64 candidate network layouts, respectively, for the one and two attachment point device cases. For one attachment point devices, comparing with the TMD, up to 34.8% performance improvement can be obtained. When considering the devices with two attachment points, the most beneficial configuration can provide almost 66% better performance than the TMD and also outperforms the TMDI with 41% performance improvement.

Data Accessibility. The source code for the results in Table 1 and Table 3 has been provided as supplementary material. Other datasets supporting this article are already in the article.

Authors' Contributions. Sara Ying Zhang led the development of the method with assistance from Yiyuan Li, Jason Zheng Jiang, Simon A. Neild and John H.G. Macdonald. All five contributed to the preparation of the manuscript.

Competing Interests. The authors declare that they have no competing interests.

Funding. This work was supported by the EPSRC, the University of Bristol: Simon A. Neild was supported by an EPSRC fellowship EP/K005375/1 and is currently supported by Programme Grant EP/R006768/1, Jason Zheng Jiang and Sara Ying Zhang are supported by an EPSRC first grant EP/P013546/1.

Acknowledgements. We gratefully acknowledge the support of our funders.

References

1. Frahm H. 1909. Device for damping vibrations of bodies.
2. Ormondroyd J, Den Hartog JP. 1928. Theory of the dynamic vibration absorber. *Transactions of the ASME*. **50**.
3. Den Hartog JP. 1956. Mechanical vibrations, 4th edn. New York, NY: McGraw-Hill. (Reprinted by Dover, New York, NY, 1985.)
4. Soong TT, Dargush GF. 1997. Passive energy dissipation systems in structural engineering. John Wiley and Sons: Chichester, West Sussex, England.
5. Den Hartog JP. 1940. Mechanical Vibration. McGraw Hill: York, PA, USA.
6. Warburton GB. 1981. Optimum absorber parameters for minimising vibration response. *Earthquake Engineering and Structural Dynamics*. **9**.
7. Ren MZ. 2001. A variant design of the dynamic vibration absorber. *Journal of Sound and Vibration*. **245**.
8. Xiang P, Nishitani A. 2013. Optimum design for more effective tuned mass damper system and its application to base-isolated buildings. *Structural Control and Health Monitoring*. **21**.
9. Marian L, Giaralis A. 2014. Optimal design of a novel tuned mass damper inerter (TMDI) passive vibration control configuration for stochastically support-excited structural systems. *Probabilistic Engineering Mechanics*. **38**.
10. Smith MC. 2002. Synthesis of mechanical networks: the inerter. *IEEE Transaction on Automatic Control*. **47**.
11. Smith MC, Wang FC. 2004. Performance benefits in passive vehicle suspensions employing inerters. *Vehicle System Dynamics*. **42**.
12. Lazar IF, Neild S, Wagg D. 2014. Using an inerter-based device for structural vibration suppression. *Earthquake Engineering and Structural Dynamics*. **43**.
13. Ikago K, Saito K, Inoue N. 2012. Seismic control of single degree of freedom structure using tuned viscous mass damper. *Earthquake Engineering and Structure Dynamics*. **41**.
14. Krenk S, Hogsberg J. 2016. Tuned resonant mass or inerter based absorbers: unified calibration with quasi-dynamic flexibility and inertia correction. *Proceedings of the Royal Society A*. **472**.
15. Zhang SY, Jiang JZ, Neild S. 2016. Optimal configurations for a linear vibration suppression device in a multi-storey building. *Structural Control and Health Monitoring*. DOI: 10.1002/stc.1887
16. Lewis TD, Jiang JZ, Neild SA, Gong C, Iwnicki SD. 2019. Using an inerter-based suspension to improve both passenger comfort and track wear in railway vehicles. *Vehicle System Dynamics*. In press.
17. Jiang JZ, Matamoros-Sanchez AZ, Goodall RM, Smith MC. 2011. Passive suspensions incorporating inerters for railway vehicles. *Vehicle System Dynamics*. **50**.
18. Wang FC, Liao MK, Liao BH, Su WJ, Chan H. 2009. The performance improvements of train suspension systems with mechanical networks employing inerters. *Vehicle System Dynamics*. **47**.

19. Giaralis A, Taflanidis A.A. 2018. Optimal tuned mass damper inerter (TMDI) design for seismically excited MDOF structures with modeluncertainties based on reliability criteria. *Structural Control and Health Monitoring*. **25**.
20. Guillemin EA. 1957. *Synthesis of Passive Networks*. New York: Wiley.
21. Foster RM. 1924. A reactance theorem. *Bell System Technical Journal*. **3**.
22. Eppstein D. 1992. Parallel recognition of series-parallel graphs. *Information and Computation*. **98**.
23. Nishizeki T, Saito N. 1974. Necessary and sufficient condition for a graph to be three-terminal series-parallel. *IEEE Transaction on Circuit and Systems*. **22**.
24. Geiger DL. 1968. *Series and parallel D-C circuits*. Cleveland Institute of Electronics.
25. Yamamoto K, Smith MC. 2016. Design of passive interconnections in tall buildings subject to earthquake disturbances to suppress inter-storey drifts. *Journal of Physics: Conference Series*. **744**.
26. Chen YT, Chai YH. 2011. Effects of brace stiffness on performance of structures with supplemental maxwell model-based brace-damper systems. *Earthquake Engineering and Structural Dynamics*. **40**.
27. Mansour N. 2011. *Search algorithms and applications*. Intech Open.
28. Firestone FA. 1933. A new analogy between mechanical and electrical systems. *Journal of Acoustic Society of America*. **4**.
29. Zhang SY, Jiang JZ, Neild SA. 2017. Passive vibration control: a structure-immittance approach. *Proceedings of the Royal Society A*. **473**.
30. Harary F. 1959. Graph theory and electric networks. *IRE Transactions on Circuit Theory*. **6**.

Appendix

A. Derivation of Immittance-Function-Matrix

Consider a 2PT1NG network shown in Figure 4(b) with velocities v_1, v_2 and forces f_1, f_2 at the two physical-terminals PT1 and PT2. Its Immittance-Function-Matrix $\mathbf{L}(s)$, relating the velocities with the forces in Laplace domain, is defined as:

$$\begin{bmatrix} F_1 \\ F_2 \end{bmatrix} = \mathbf{L}(s) \begin{bmatrix} V_1 \\ V_2 \end{bmatrix}, \quad (\text{A.1})$$

where $\mathbf{L}(s)$ is a 2×2 matrix, made up of four immittance functions, denoted as $\mathbf{L}(1, 1)$, $\mathbf{L}(1, 2)$, $\mathbf{L}(2, 1)$ and $\mathbf{L}(2, 2)$.

For the generic IF-Network, $\mathbf{L}_1(s)$ shown in Table 2, the equation of motion, in Laplace domain, can be derived as:

$$F_1 = sY_3(s)(V_1 - V_m), \quad F_2 = sY_2(s)(V_2 - V_m), \quad \text{and} \quad msV_m = F_1 + F_2, \quad (\text{A.2})$$

where V_m is the velocity of the reaction mass with its value defined as positive to the right. By expressing V_m as a function of V_1, V_2 , the IF-Matrix of the generic IF-Network, $\mathbf{L}_1(s)$, can be written as:

$$\mathbf{L}_1(s) = \frac{Y_2(s)Y_3(s)}{Y_2(s) + Y_3(s) + ms} \begin{bmatrix} \frac{(Y_2(s) + ms)}{Y_2(s)} & -1 \\ -1 & \frac{(Y_3(s) + ms)}{Y_3(s)} \end{bmatrix}. \quad (\text{A.3})$$

The IF-Matrix of the generic IF-Network for the $R = 2$ case, shown in Table 2, can then be obtained by replacing ms in (A.3) with $Y_m(s)$, to give

$$\mathbf{L}_2(s) = \frac{Y_2(s)Y_3(s)}{Y_2(s) + Y_3(s) + Y_m(s)} \begin{bmatrix} \frac{(Y_2(s) + Y_m(s))}{Y_2(s)} & -1 \\ -1 & \frac{(Y_3(s) + Y_m(s))}{Y_3(s)} \end{bmatrix}. \quad (\text{A.4})$$

where

$$Y_m(s) = Y_1(s)ms / (Y_1(s) + ms) \quad (\text{A.5})$$

represents a mass connected in series with the IF-Block $Y_1(s)$. Built on (A.4), the IF-Matrix of the generic IF-Networks, $\mathbf{L}_R(s)$, for the even R case ($R \geq 3$, see the left-hand side of Table 2), can be obtained by a parallel connection between $\mathbf{L}_{R-1}(s)$ and $Y_{\frac{3R-1}{2}}(s)$, given by

$$\mathbf{L}_R(s) = \left(\mathbf{L}_{R-1}(s) + Y_{\frac{3R-1}{2}}(s) \begin{bmatrix} 1 & -1 \\ -1 & 1 \end{bmatrix} \right) \quad (\text{A.6})$$

For the series connection between $\mathbf{L}_{R-1}(s)$ and two IF-Blocks $Y_{\frac{3R}{2}-1}(s)$, $Y_{\frac{3R}{2}}(s)$ (see the right-hand side of Table 2), the IF-Matrix can be formulated by first deriving $\mathbf{L}'_R(s)$, using

$$\mathbf{L}'_R(s) = \frac{1}{Y_{\frac{3R}{2}-1}(s) + \mathbf{L}_{R-1}(2,2)} \left(Y_{\frac{3R}{2}-1}(s)\mathbf{L}_{R-1}(s) + \begin{bmatrix} |\mathbf{L}_{R-1}(s)| & 0 \\ 0 & 0 \end{bmatrix} \right) \quad (\text{A.7})$$

and then substituting this into

$$\mathbf{L}_R(s) = \frac{1}{Y_{\frac{3R}{2}}(s) + \mathbf{L}'_R(1,1)} \left(Y_{\frac{3R}{2}}(s)\mathbf{L}'_R(s) + \begin{bmatrix} 0 & 0 \\ 0 & |\mathbf{L}'_R(s)| \end{bmatrix} \right) \quad (\text{A.8})$$

B. 2PT1NG IF-Network possibilities with $R = 1, 2, 3, 4$

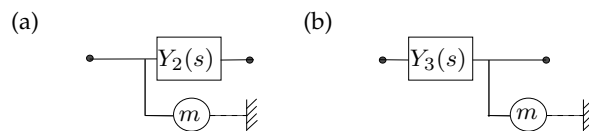


Figure 15: The two IF-Network cases for $R = 1$.

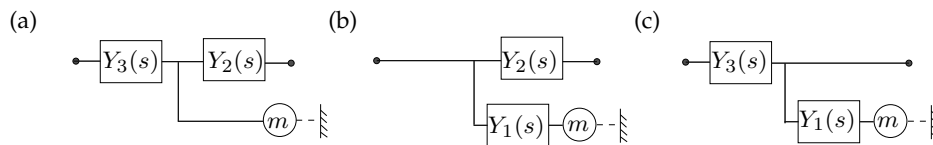


Figure 16: The three IF-Network cases for $R = 2$.

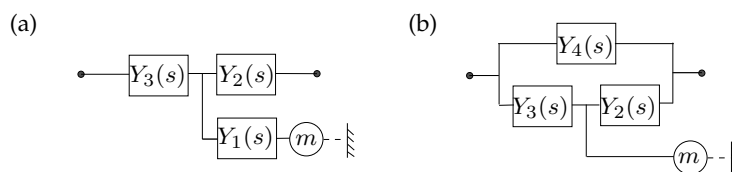


Figure 17: The two IF-Network cases for $R = 3$.

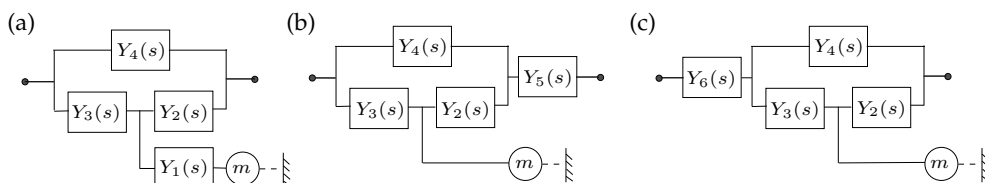


Figure 18: The three IF-Network cases for $R = 4$.